THE RESPONSE OF SCREW CORNER JOINTS MANUFACTURED OF HONEYCOMB PANELS TO CHANGES IN RELATIVE AIR HUMIDITY

Smardzewski Jerzy^{1,2}, Tokarczyk Maciej¹, Giedrius Pilkis²

- ¹ Poznan University of Life Sciences, Faculty of Forestry and Wood Technology, Wojska Polskiego 28, Poznan, Poland
- ² Vilnius Academy of Arts, Maironio g. 3, LT-01124 Vilnius, Lithuania

Link to this article: https://doi.org/10.11118/978-80-7701-044-3-0055

Abstract

Honeycomb panels are an attractive material for furniture production. However, their usefulness in industrial practice depends on the technological quality of corner joints and the effect of temperature and relative humidity changes on the stiffness and strength of these joints. This work made corner joints from 37 mm thick honeycomb panels. A screw confirmat type was used for the connection. It was experimentally determined to what extent a change in air relative humidity from 40% to 85% will affect the strength and stiffness of corner joints. Numerical models were developed to predict the behavior of joints in variable climatic conditions. It was shown that an increase in air humidity reduces the stiffness and strength of joints. However, in conditions of extreme humidity of 85%, the stiffness and strength of joints are still acceptable compared to dry conditions (40%). Numerical models allow for correct estimation of the quality of joints.

Keywords: honeycomb, screw joint, air humidity, strength, stiffness, FEM

INTRODUCTION

An important reason for using lightweight panels in the furniture industry is to protect the environment and reduce production costs (Feifel, Poganietz, Schebek, 2013; Nordvik, Broman, 2005). Popular wood materials such as PB particleboard, mediumdensity MDF, and high-density HDF are widely used in practice due to their favorable strength-to-low density ratio (Smardzewski, Slonina, Maslej, 2017). More competitive, however, are lightweight panels. Their low weight is their most significant asset (Librescu, Hause, 2000; Shalbafan et al., 2012), especially in furniture manufacturing (Allen, 1969; Smardzewski 2013). Wood-based cellular panels, however, are more vulnerable to climatic conditions changes at their sites of use (Smardzewski, Slonina, Maslej, 2017; Nilsson, Ormarsson, Johansson, 2017). This is due to the function of the rooms, such as the kitchen, bathroom or living room, and also the world's climatic zones. In order to make effective use of this raw material, their suitability for designing durable and long-lasting furniture joints must be carefully considered (Carll, Wiedenhoeft, 2009; Smardzewski, Łabęda, 2018). To date, the stiffness and strength of cellular board joints have been tested under residential conditions, that is, at a relative humidity and air temperature of approximately 65% and 21°C (Kasal *et al.*, 2008; Tankut, 2009; Kasal *et al.*, 2014).

This study aimed to increase knowledge of the effect of climate change (relative humidity and air temperature) on the strength and stiffness of corner joints of lightweight panels assembled with confirmat bolts. In addition, the study aimed to determine the failure mode of the connections using the finite element method. This knowledge can be used to optimise the design of lightweight furniture.

MATERIALS AND METHODS

For the tests, corner joints were made of lightweight panels with a thickness of t_p =37 mm (Fig. 1). The length of the joint arms L_e was equal to 150 mm, and the joint width L = 390 mm. The facings were made of high-density fibreboard (HDF) with a thickness of t_f = 2.5 mm, while the core was made from particle board (PB) and paper honeycomb (PP) with a thickness of t_c = 32 mm. The core had a frame structure (Fig. 2). The frame around the perimeter of the specimen was made from strips of particleboard with a thickness of t_s = 12 mm. Reinforcing blocks

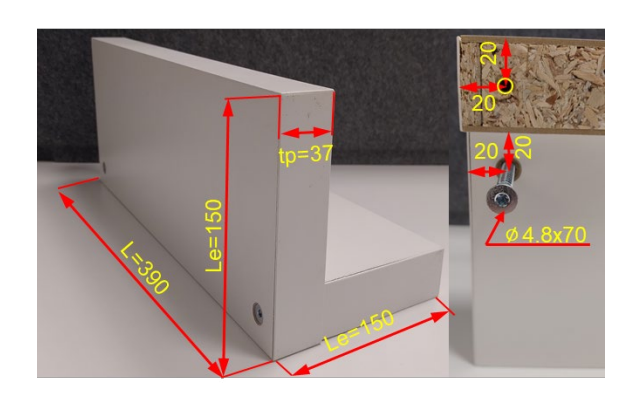




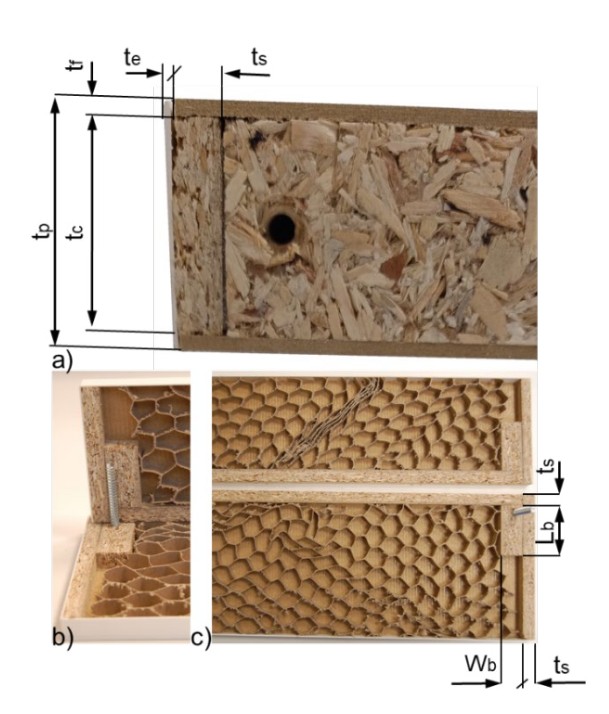


Open access. This work is licensed under the terms of the Creative Commons Attribution-NonCommercial 4.0 International (CC BY-NC 4.0) https://creativecommons.org/licenses/by-nc/4.0/deed.en

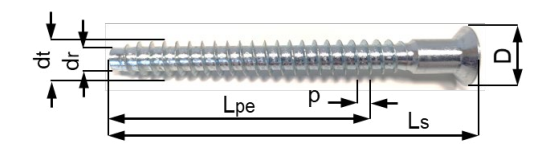
with a width of $W_b = 24 \,\mathrm{mm}$ and length $L_b = 50 \,\mathrm{mm}$. The thickness of the block corresponded to the thickness of the cellular board core. The core filling was a honeycomb made from Testliner-2 paper (HM Technology, Brzozowo, Poland)) with a thickness of $t = 0.23 \,\mathrm{mm}$. The hexagonal cells of the core were characterised by a length of L_c =31 mm, width S_c = 26 mm, double wall length $h_c = 8 \,\mathrm{mm}$ and free wall length $l_c = 13 \,\mathrm{mm}$. The average value of the cell wall angle was equal to φ = 39.4 degrees (0.688 rad). The cladding and core elements were glued together using PVAc Woodmax FF 12.47 class D2 adhesive applied at approximately 110 g/m² (Synthos Adhesives, Oświęcim, Poland). The table top was edged on narrow surfaces with ABS edging (Acrylonitrile Butadiene Styrene, Rehau Sp. z o.o. Baranowo, Poland) using Jowat 280.30 hot-melt adhesive (Jowat Sp. Z o.o., Sady, Poland). The edge banding used was $t_{o} = 1$ mm.



1: Samples dimensions



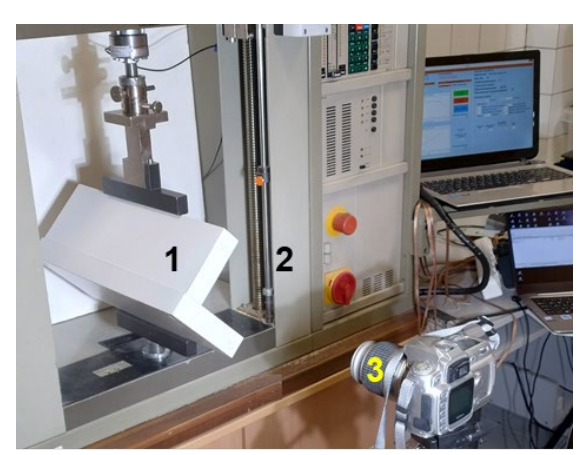
2: Cross section of joint

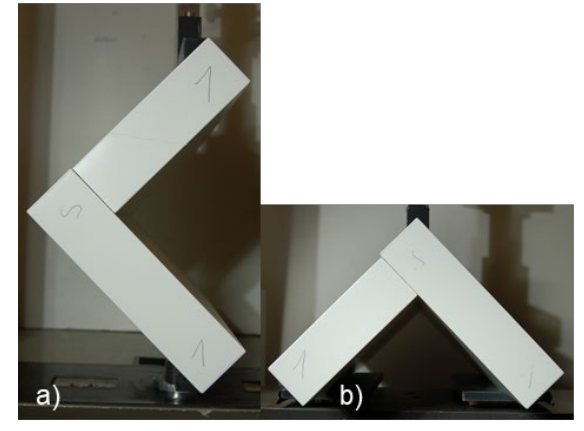


3: Screw dimensions

The joints were connected using confiirmate screws with a length of L_s = 70 mm, thread diameter $d_r = 7$ mm, core diameter $d_r = 4.8$ mm and a thread length embedded in the plate to a depth of L_{pe} = 32 mm. The pitch of the thread was p_e =2.4 mm, and the head diameter $D = 9 \,\mathrm{mm}$ (Fig. 3). The joints were decided to be subjected to compressive and tensile loading under varying climatic conditions. For this purpose, a laboratory test rig was prepared to determine the stiffness and strength of the corner joints of box furniture in the shortening and opening test (Fig. 4). A climate chamber was also prepared to simulate dry conditions (D) (temperature 26°C and relative humidity 40%) and wet conditions (W) (temperature 28°C and relative humidity 85%). Ten joints were prepared for each sample, for a total of forty samples.

The prepared specimens were short-circuited and pulled apart (Fig. 4) on a Zwick 1445 universal testing machine. During loading, the displacements





4: Universal testing maschine: 1) sample, 2) test machine, 3) digital camera. Compression a) and tension b) test

were recorded with an accuracy of 0.01 mm, and the force was measured with a resolution of 0.01 mm. δP were recorded with an accuracy of 0.01 mm and the force with an accuracy of 0.01 N. P with an accuracy of 0.01 N. Testing continued until the specimen failed with a load drop of at least 100 N or until a displacement of 10 mm was achieved.

The strength of the joints was determined by comparing the maximum bending moments that caused the failure of the joint. For joints subjected to compression, the strength M_c is given by the formula:

$$M_c = P\alpha'$$

and for tensiled joints, the strength $M_{\scriptscriptstyle T}$ is determined by the formula:

$$M_{\scriptscriptstyle T}$$
 = Pe'

In the compression (closing) test, the joint stiffness K_c was calculated from the equation:

$$K_C = \frac{M_C}{\Delta \varphi} = \frac{P\alpha'}{\Delta \varphi}$$
 [Nm/rad]

where:

$$\Delta \varphi = \frac{\pi}{90} \left(\alpha t g \left(\frac{\sqrt{2}}{2} \frac{L_e}{\alpha'} \right) - \alpha \sin \left(\frac{\sqrt{2}}{2} \frac{L_e - \delta P_{0.4} P_{max}}{\sqrt{t_p^2 + (L_e - t_p)^2}} \right) \right)$$

$$\alpha' = \frac{\sqrt{2}}{2} L_e - \sqrt{2t_p}$$

In the tension (opening) test, the stiffness of the joint K_{τ} was calculated from the equation:

$$K_T = \frac{M_T}{\Delta \varphi} = \frac{Pe'}{\Delta \varphi}$$
 [Nm/rad]

where:

$$\Delta \varphi = \frac{\pi}{90} \alpha t g \left(\frac{\sqrt{\frac{1}{2} (L_e - t_p)^2 (L_e + t_p)^2 - ((L_e + t_p) - \delta P_{0.4} P_{max})^2}}{(L_e + t_p) - \delta P_{0.4} P_{max}} \right)$$

$$-2\alpha tg\left(\frac{(L_e - t_p)}{(L_e + t_p)}\right)$$

$$e' = \frac{\sqrt{2}}{2} (L_e - t_p)$$

Numerical Model

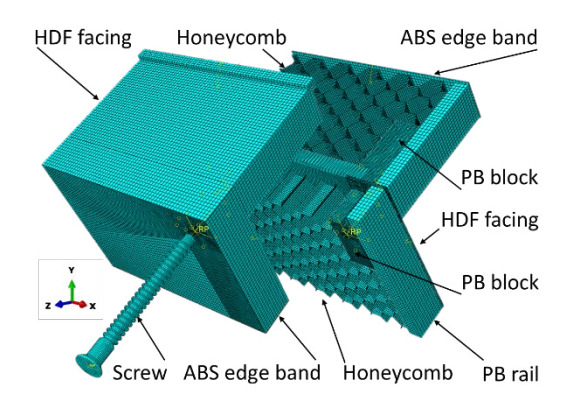
It was also decided to determine the strength of the joint by numerical calculations using the finite element method. The structure of the model corresponded to the structure shown in Fig. 2. First, realistic computer models of the connections were made in Autodesk Inventor (Autodesk, Warsaw, Poland). Then, taking into account the symmetry of the structure, numerical models of the screw connections were developed (Fig. 5).

An 8-node linear brick, reduced integration, hourglass control element type C3D8R was used for PB, HDF, PP, ABS materials (mesh density from 0.1 mm to 3 mm). For the screw and thrust, A4-node 3-D bilinear rigid quadrilateral elements type R3D4 (mesh density from 0.83 to 3 mm) were used. Between the surfaces of the facings, slats (rails) and cores, a "tie" type interaction was used (Smardzewski, Tokarczyk 2024). A contact with a friction coefficient of 0.15 and 0.13, respectively, was used between the surface of the screw and the surfaces of the holes in the PB particleboard and HDF board. A contact with a friction coefficient of 0.23 was used for the contact surfaces of the joint arms.

Based on the results of our own research, Tab. I summarises the physical and mechanical properties of the materials used to create the joints under dry conditions, temperature and relative humidity of 20C, 40% respectively (Krzyżaniak, Smardzewski, 2021; Kasal *et al.*, 2023). It was assumed that

I: Physical-mechanical properties of the materials used for the joints. Standard deviation in brackets, MC (%) moisture content, D (kg/m^2) density, v Poisson's ratio, G (MPa) shear modulus, E (MPa) linear modulus, E (MPa) static yield strength (E) tay et al., 2019; Krzyżaniak, Smardzewski, 2021; Kasal et al., 2023)

Property	Unit		PB		HDF	ABS	Steel
		t = 32	$t_{top} = 3$	$t_{mid} = 26$	<i>tf</i> = 2.5	$t_{_{e}}$ = 1.0	-
MC	%	6.18 (0.08)	5.2 (0.09)	6.54 (0.1)	5.07 (0.11)	-	-
D	kg/m³	649 (7)	882 (4.8)	541 (5)	966 (62)	1 100 (-)	70 860 (-)
υ			0.29		0.30	0.30	0.30
G	МРа	991 (112)	1298 (85)	682 (72)		E/2(1 + v)	
E		2 556 (290)	3 350 (220)	1760 (185)	5 190 (67)	16 000 (-)	210 000 (-)
R		10.9 (1.8)	14.1 (2.1)	7.8 (1.7)	32.3 (1.83)	58.0 (-)	430 (-)



5: Mesh model of joint

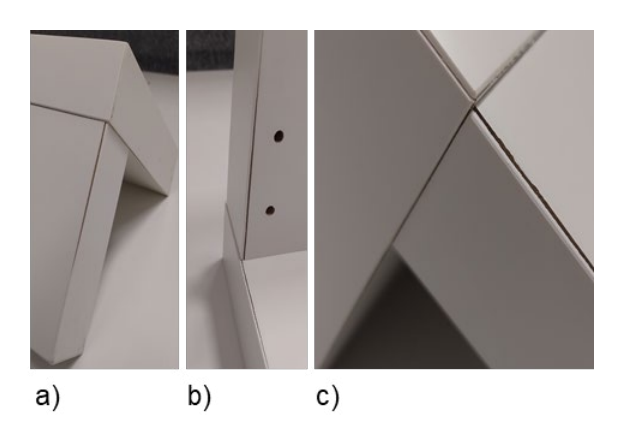
particleboards are three-layer systems. Therefore, the elastic properties of the outer layers with a thickness of t_{top} =3 mm and middle layers with a thickness of t_{mid} = 26 mm. The properties of ABS edging strips are given based on the work of (Lay *et al.*, 2019).

All numerical computations were performed at the Poznań Supercomputing and Networking Center (PSNC) using the Eagle computing cluster. The finite element analysis was conducted using Abaqus/Explicite v.6.14-2 (Dassault Systemes Simulia Corp., Waltham, Ma, USA).

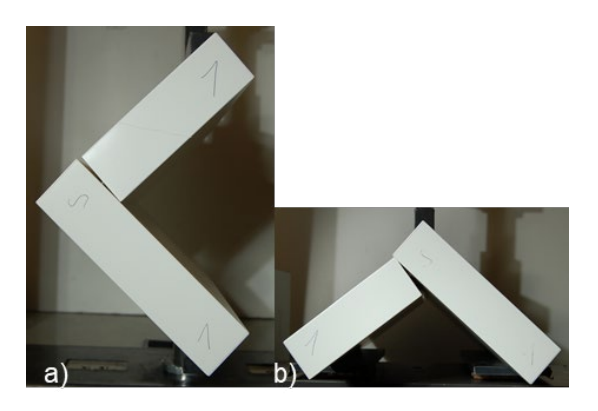
RESULTS AND DISCUSSION

Experimental Part

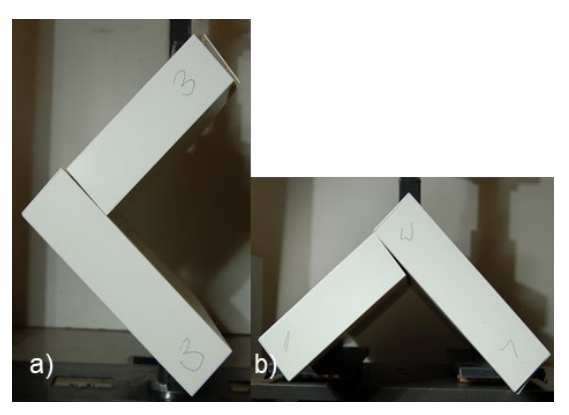
As the samples were divided into two groups, air-conditioned in dry conditions of the production hall (D) and conditions with increased temperature and relative humidity (W), they were visually inspected, and the most common air-conditioning-induced damages were selected (Fig. 6). The most common damages to the furniture joints included peeling off of the edging on the narrow surfaces of the panel elements. The peeling off caused exposure of the particleboard and penetration of water vapour deep into the core of the particleboard.



6: The most common cases of damage of panels after wetting: a,b) butt member, c) butt and face members



7: Damage of dry joints under a) compression, b) tension

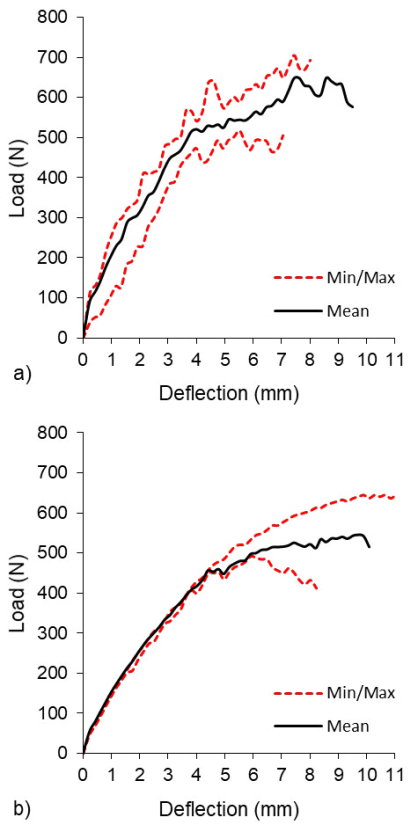


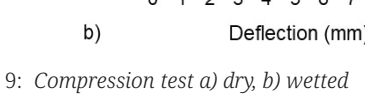
8: Damage of wett joints under a) compression, b) tension

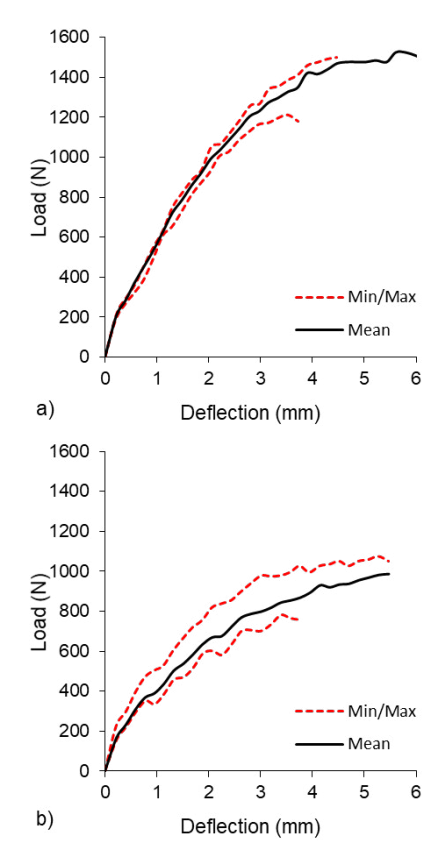
During the tests of furniture connections, the force value was recorded P with an accuracy of 0.01 N and the displacement δP in the direction of force application P with an accuracy of 0.01 mm. The stiffness K_C , K_T of the joints was determined moistened under dry conditions (D) T = 26C and H = 40%, and the stiffness of the joints K_C , K_T conditioned under wet conditions (W) T = 28C and H = 85%. Characteristic failures of dry joints are shown in Fig. 7, and failures of wet joints in Fig. 8.

Fig. 9 shows the average failure forces of the joints in the closing test. The maximum failure force for dry-conditioned joints (D) was 648 N, while for wetconditioned joints (W) it was 541 N, respectively, at a similar displacement. It was noted here that the dry joints (D) were not homogeneous and provided different force values throughout the closing test (Fig. 9a). Wet joints (W) in the displacement range up to 4 mm showed regularity of results (Fig. 9b). Beyond a displacement of 4 mm, the force values started to vary and at a maximum displacement of about 10 mm, the force differences were as high as 244 N.

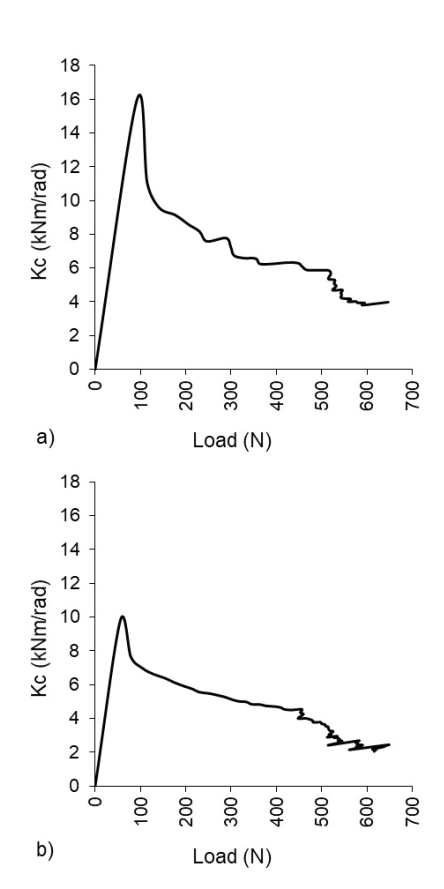
The joints also differed in the slope of the curve relative to the horizontal axis. This resulted in a change in the stiffness of these joints. Fig. 10 shows that the maximum stiffness of the dry joints (D) subjected to a closing force of about 80 N was equal to 15.8 Nm/rad, while the maximum stiffness of the wet joints (W) was 9.8 Nm/rad. However, it should



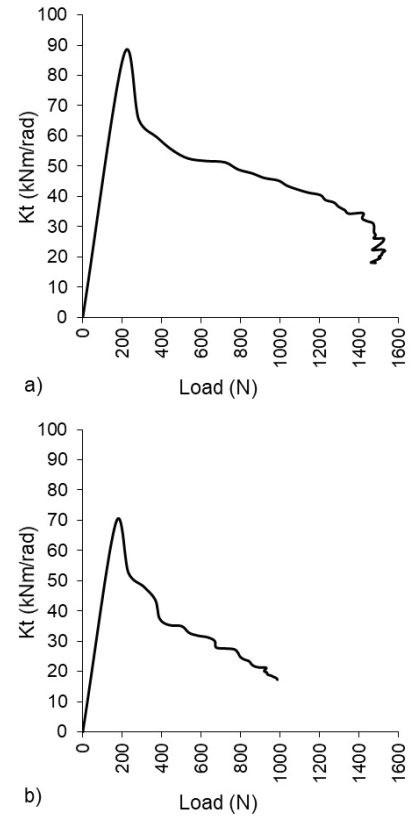




11: Tension test a) dry, b) wetted



10: Compression test a) dry, b) wetted



12: Tension test a) dry, b) wetted

be noted that as the load increased, the stiffness of both connections decreased. For forces of $200\,\mathrm{N}$, $300\,\mathrm{N}$ and $400\,\mathrm{N}$, the ratios were equal to 8.6 and 5.9, 7.2 and 5.1, 6.2 and 4.6 (Nm/rad) respectively.

Fig. 11, on the other hand, shows the average failure forces of the joints in the opening test. In the case of dry-conditioned joints (D), the maximum failure force was 1524N, while in the case of wetconditioned joints (W) it was 986 N, respectively, at a similar displacement. It was noted here that the wet joints (W) were not homogeneous this time and provided different force values throughout the dilation test (Fig. 9b). Dry joints (D) in the range of displacements up to 3 mm showed a high repeatability of results (Fig. 11a). Beyond a displacement of 3 mm, the force values started to vary, and at a maximum displacement of about 4.5 mm, the force differences were as high as 320 N. As in the case of tension, the joints also differed in the slope of the curve relative to the horizontal axis. This resulted in a change in the stiffness of these joints.

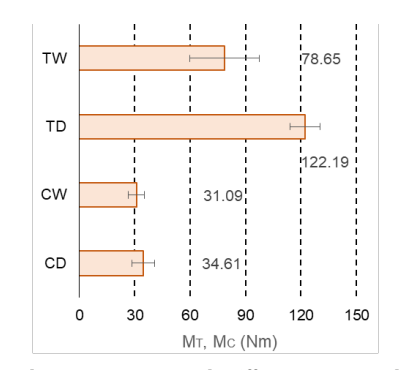
Fig. 12 shows that the maximum stiffness of the dry joints (D) subjected to a force of about 190 N was equal to 86.3 Nm/rad, while the maximum stiffness of the wet joints (W) was 68.8 Nm/rad. It should also be noted here that as the load increased, the stiffness of both joints decreased. The ratios for 400 N, 600 N, and 800 N forces were 77.5 and 37.5, 51.7 and 31.8, 48.9 and 24.8 (Nm/rad), respectively.

It can also be seen from Fig. 10 and 12 that wet conditioning reduces the stiffness of the diverging joint (T) from 86.31 Nm/rad to 68.64 Nm/rad. The change is from 15.9 Nm/rad to 9.8 Nm/rad during closing.

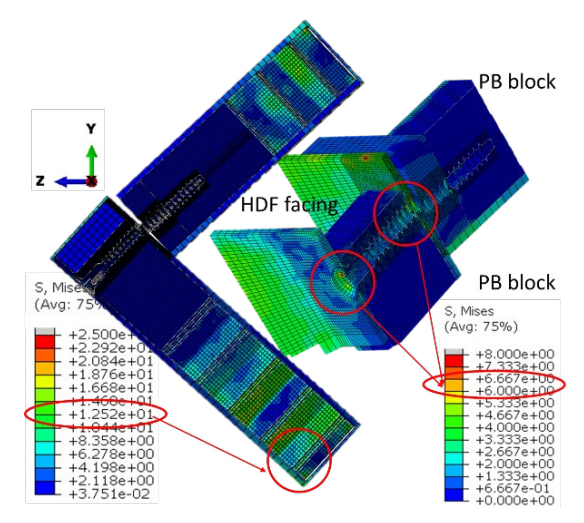
The differences in the strength and stiffness of the joints are illustrated in Fig. 13, which shows that changing the conditioning conditions of the joints significantly affects their strength in the dilation test (T). In this case, the strength of the connections decreases from 122.19 Nm to 78.65 Nm. For joints subjected to compression (C), the strength of the connections decreases from 34.61 Nm to 31.09 Nm.

Numerical Part

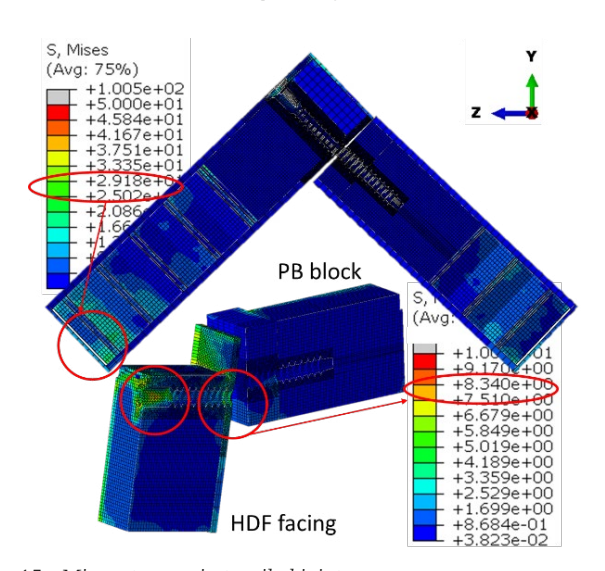
The numerical calculations were designed to show the characteristic damage at the screw and socket contact points in the particleboard. It can be seen



13: Strength $(M_T,\ M_c)$ a) and stiffness $(K_T,\ K_c)$ b) of joits, W - wett, D - dry, T - tension, C - compression



14: Mises stresses in compressed joints



15: Mises stresses in tensiled joints

from Fig. 14 that during short-circuiting, the highest stresses, with a value of 12.52 MPa, are concentrated on the edges at the point of load application and the point of support. These stresses do not exceed the strength of the weakest material in the structure at 14.1 MPa (Tab. I). At the bolt and chipboard block junction, the stresses reach a value of 6.67 MPa. These values do not exceed the strength of the central part of the particleboard of 7.8 MPa.

Fig. 15 illustrates the stresses in joints subjected to tension. The highest stresses, with a value of 29.18 MPa, are concentrated on the edges at the point of load application and the point of support. The value of these stresses exceeds the chipboard strength of 14.1 MPa. At the joint between the screw and the particleboard blocks, the stresses reach a value of 8.34 MPa. These values exceed the strength of the central part of the particleboard 7.8 MPa.

Numerical tests have shown that the strength of the connections is sufficiently effective for use in industrial solutions.

CONCLUSION

The experimental study involved determining the effect of temperature and relative humidity changes on the stiffness and strength of corner joints made from 37 mm thick lightweight panels. Confirmat screws were used for the joints. Experimentally, it was shown that changing the temperature and relative humidity of the air from 26C, 40% to 28C, 85% significantly affected the strength and stiffness of the corner joints. When the specimens are humidified, their strength decreases by 10.2% in the short-circuit test. During dilation, the strength decreases by 35.6%. Moistening the specimens also reduces the stiffness of the joints by 38.4% and 20.5% for short-circuited and open-circuited joints, respectively. However, the numerical models developed confirm that the strength of the connections is still acceptable under extreme loading conditions. Slight failures only occur in non-visible areas at the interface between the screw and the thread formed in the chipboard.

Acknowledgements

This project has received funding from the Research Council of Lithuania (LMTLT), agreement No: S-A-UEI-23-3.

REFERENCES

- [1] ALLEN, Howard Georg. 1969 Effect of cell-wall angle on the uniaxial crushing behaviour of paper hexagonal honeycombs. New York: Pergamon Press. ISBN 9789532920314
- [2] CARLL, Charles; WIEDENHOEFT, Alex C. 2009. Moisture-related properties of wood and the effects of moisture on wood and wood products. In: *Moisture Control in Buildings: The Key Factor in Mold Prevention*. ASTM Manual. 2nd Edition. West Conshohocken, PA: ASTM International, c2009. Chapter 4, p.54–79.
- [3] FEIFEL, Silke, POGANIETZ, Witold-Roger; SCHEBEK, Liselotte. 2013. The utilization of light weight boards for reducing air emissions by the German wood industry a perspective? *Environmental Sciences Europe*. 25, 5. https://doi.org/10.1186/2190-4715-25-5
- [4] HARKATI, A. et al. 2020. In-plane elastic constants of a new curved cell walls honeycomb concept. *Thin-Walled Structures*. 149, 106613. https://doi.org/10.1016/j.tws.2020.106613
- [5] KASAL, A. *et al.* 2008. Effects of screw sizes on load bearing capacity and stiffness of five-sided furniture cases constructed of particleboard and medium density fiberboard. *Forest Products Journal*. 58(10), 25–32.
- [6] KASAL, A. *et al.* 2014. Effect of material properties and anchorage location on load-bearing capacity of screw-connected and hung cabinets. *Wood and Fiber Science*. 46(1), 1–10.
- [7] KASAL, Ali *et al.* 2023. Analyses of L-Type Corner Joints Connected with Auxetic Dowels for Case Furniture. *Materials*. 16(13), 4547. https://doi.org/10.3390/ma16134547
- [8] KRZYŻANIAK, Łukasz; MARDZEWSKI, Jerzy. 2021. Impact damage response of L-type corner joints connected with new innovative furniture fasteners in wood-based composites panels. *Composite Structures*. 255, 113008. https://doi.org/10.1016/j.compstruct.2020.113008
- [9] LAY, Makara *et al.* 2019. Comparison of physical and mechanical properties of PLA, ABS and nylon 6 fabricated using fused deposition modeling and injection molding. *Composites Part B: Engineering.* 176, 107341. https://doi.org/10.1016/J.COMPOSITESB.2019.107341
- [10] LIBRESCU, Liviu; HAUSE, Terry. 2000. Recent developments in the modelling and behavior of advanced sandwich constructions: A survey. *Composite Structures*. 48(1-3), pp. 1–17. https://doi.org/10.1016/S0263-8223(99)00068-9
- [11] NILSSON, Jonaz, ORMARSSON, Sigurdur; JOHANSSON, Jimmy. 2017. Moisture-related distortion and damage of lightweight wood panels-experimental and numerical study. *Journal of the Indian Academy of Wood Science*. 14(2), 99–109. https://doi.org/10.1007/s13196-017-0193-y
- [12] NORDVIK, Enar; BROMAN, N. Olof. 2005. Visualizing wood interiors: a qualitative assessment of what people react to and how they describe it. *Forest Products Journal*. 55(2), 81–86.
- [13] SHALBAFAN, A. *et al.* 2012. Comparison of foam core materials in innovative lightweight wood-based panels. *European Journal of Wood and Wood Products*. 70(1–3), 287–292. https://doi.org/10.1007/s00107-011-0552-0
- [14] SMARDZEWSKI, J. 2013. Elastic properties of cellular wood panels with hexagonal and auxetic cores. *Holzforschung*. 67(1), 87–92. https://doi.org/10.1515/hf-2012-0055
- [15] SMARDZEWSKI, J.; ŁABĘDA, Karol. 2018. Mechanical and Hygroscopic Properties of Longitudinally- Laminated Timber (LLT) Panels for the Furniture Industry. *BioResources*. 13(2017), 2871–2886. https://doi.org/10.15376/biores.13.2.2871-2886

- [16] SMARDZEWSKI, Jerzy; MAJEWSKI, Adam. 2015. Mechanical properties of auxetic honeycomb core with triangular cells. In: *25th International Scientific Conference New materials and technologies in the function of wooden products*, pp. 103–112. ISBN 9789532920345
- [17] SMARDZEWSKI, Jerzy, SŁONINA, Michał; MASLEJ, Michał. 2017. Stiffness and failure behaviour of wood-based honeycomb sandwich corner joints in different climates. *Composite Structures*. 168, 153–163. https://doi.org/10.1016/j.compstruct.2017.02.047
- [18] SMARDZEWSKI, Jerzy; TOKARCZYK, Maciej. 2024. Lightweight honeycomb furniture panels with discreetly located strengthening blocks. *Composite Structures*. 331, 117927. https://doi.org/10.1016/J.COMPSTRUCT.2024.117927
- [19] TANKUT, Nurgul. 2009. Effect of various factors on the rigidity of furniture cases. *African Journal of Biotechnology*. 8(20), 5265–5270.

Reviewer Dr. Manja Kitek Kuzman, PhD – University of Ljubljana (Slovenia)

Contact information Smardzewski Jerzy: jsmardzewski@up.poznan.pl